P- and S-wave Seismic Reflection and Refraction Measurements at CCOC

By Robert A. Williams, William J. Stephenson, Jack K. Odum, and David M. Worley

This paper is an extract from

Asten, M.W., and Boore, D.M., eds., Blind comparisons of shear-wave velocities at closely spaced sites in San Jose, California: U.S. Geological Survey Open-File Report 2005-1169. [available on the World Wide Web at http://pubs.usgs.gov/of/2005/1169/].

2005

U.S. DEPARTMENT OF THE INTERIOR
U.S. GEOLOGICAL SURVEY

U.S. Geological Survey, Denver Federal Center, MS 966, Box 25046, Denver, CO 80225

Abstract

P- and S-wave seismic reflection/refraction surveys conducted about 200 m southeast of the CCOC drill hole reveal 8 distinct S-wave layers, including two velocity inversions (high-to-low velocity layer boundaries) and 4 P-wave layers. The S-wave velocity profile submitted for comparison with other methodologies was determined using only reflection data and these velocities range from about 150 m/s at the surface to about 500 m/s at the maximum imaged depth of 80 m. The V_{s30} value from these data is 220 m/s. P-wave velocities range from about 280 m/s at the surface to about 2080 m/s at 15 m depth.

Introduction

This paper summarizes our results from near the Coyote Creek Outdoor Classroom (CCOC) site using reflection/refraction methodology to measure sedimentary layer thicknesses and P- and S-wave seismic velocities (V_p and V_s) in the upper 80 m. These data were collected on April 9, 2003. To accommodate the length of the geophone array needed for this study, the array was located on the eastern edge of William St. Park about 200 m southeast of the CCOC drill hole (Fig. 1). The location of our seismic profile is near the location of several of the other studies described elsewhere in this report (see Table 1 for latitude/longitude coordinates). Other studies that have used similar methodology to acquire V_s and V_p data in noisy urban areas are Campbell and Duke (1976), King *et al*. (1990), Williams *et al*. (1994), and Harris *et al*. (1994).

Seismic reflection/refraction imaging has successfully been used in the oil industry to detect buried hydrocarbon traps for about 85 years (Dobrin, 1976). Use of surface reflection/refraction methods to characterize the near surface, generally the upper 100 m, is a much younger application, but is still based on about two decades of concentrated research refining these techniques in field and lab studies. As summarized by Steeples (1998), high quality images of the upper 100 m of ground using reflection/refraction imaging methods have been described in dozens of papers since the early 1980's. For high-resolution *P*-wave seismic-reflection data acquired with much shorter geophone intervals than used in this study, minimum imaging depths have decreased and resolution limits of thin beds have increased to where layers as shallow as 1 m and beds as thin as 0.1 m can be detected under the right conditions (Steeples, 1998). Because similar seismic sources and sensors are used, minimum imaging depths and resolution limits for seismic-refraction data are comparable to those of seismic-reflection data. Also, in many reflection/refraction studies the interpreted layer boundaries have been corroborated by the stratigraphy interpreted from borehole data (e.g., Luzietti *et al*., 1992; Miller *et al*., 1995; Liberty, 1998). These studies show that reflection/refraction data have become a valuable tool in near-surface studies.

A previous study comparing reflection/refraction and downhole data from Williams and others (2003) shows that, despite significant differences in the subsurface area sampled by these two methods, similar velocity structures are determined. These

velocity structures are similar in terms of overall velocity trends determined by visual inspection of velocity-depth profiles, V_{s30} (for NEHRP site categories), and calculated amplification ratios. The main differences in velocity-depth data between the two methods are that the downhole data tend to expose a slightly greater number of distinct velocity layers over the upper 30 m and a greater number of velocity inversions. We also show that it is unlikely that surface reflection/refraction data will duplicate the downhole velocity log determined by measurements every 1 to 3 meters.

Some advantages of the surface reflection/refraction method over procedures based on drilling are that it: 1) is less invasive with fewer permitting and environmental complications, 2) is faster (especially when compared to the complete drilling operation, typically, about 2 sites per day can be acquired), 3) offers a more areally extensive sample of the subsurface, 4) in some cases, can directly detect potentially strong site resonances through reflection travel times (Williams *et al*., 2000), and 5) is less costly by about a factor of 3 to 4. It costs about $1000 for each reflection/refraction site, including data acquisition and processing, as compared to a 30-m deep borehole geologically logged by a continuous flight auger and then measured geophysically by downhole methods (J. Tinsley, personal commun., 2001). Some of the disadvantages of using surface reflection/refraction methods versus downhole methods are: 1) velocity inversions can go undetected, 2) there is sometimes a limited depth range due to space and energy source restrictions, 3) no sample of subsurface material is taken and no in-situ testing is possible, 4) data analysis is probably more complicated because it requires analysis and interpretation of reflection and refraction phases rather than just 1st-arrival travel times, and 5) ambient noise probably has a larger degrading effect on the reflection/refraction data than on downhole data because source signal is more strongly attenuated at the maximum source-receiver offset distances due to the generally greater source-receiver distances used in reflection/refraction methods. Usually, the ambient noise can be sufficiently attenuated or removed by bandpass filtering. We have shown that the first disadvantage listed above can sometimes be avoided or have a reduced impact by incorporating reflection data and recognizing velocity inversion indicators in the refracted first-arrival pattern. Disadvantages 2 and 3 are not critical to velocity determinations and also may be outweighed by some of the reflection/refraction advantages.

Seismic Data Acquisition

Shear-wave (S-wave) data were recorded on a 24-bit seismograph using a linear array of 60, 4.5-Hz horizontal-component geophones spaced 3.0 m apart and oriented perpendicular to the profile direction. The *S*-wave seismic source consisted of a wooden timber with steel caps placed on pavement or soil beneath the wheels of the vehicle at right angles to the direction of the profile. Reversed polarity seismic energy was produced by striking opposite ends of the timber with a 4-kg sledgehammer. Eight hammer impacts were stacked together at each endpoint of the array to form a set of reversed seismic *S*-wave profiles 177 m in length.

Compressional P-wave velocity data were recorded using an in-line spread of 60 8-Hz, vertical-component geophones spaced at 3 m intervals. P-wave energy was stacked together from 8 impacts generated by vertically striking a steel plate with a 250-kg

elastically accelerated weight drop. Recording parameters for both S-wave and P-wave surveys are listed in Table 1.

Seismic Data Processing and Interpretation

We interpreted the refraction data using the slope-intercept method as described by Mooney (1984), which assumes continuous, but potentially dipping, layers across the length of the spread, while seismic reflections were interpreted separately using a hyperbolic curve-fitting utility within the computer program ProMAX® (Landmark Graphics Corp., 2002). For this study we averaged the resultant depths to produce single set of depth-velocity pairs that represent the site in the middle of the geophone spread. The seismic profile was located on a generally flat surface so no elevation corrections were needed. For the reflection data we determined their moveout velocities and picked the zero-offset travel times to obtain depth measurements using the Dix equation as described by Dobrin (1976). To get an estimate of the error bounds for both the reflection and refraction data, we determined that by intentionally mis-positioning the line fit from the preferred slopes a tolerable amount, the maximum possible velocity variation is about 15 percent. Given the recorded dominant S-wave bandwidth of about 20-60 Hz and the interpreted seismic velocity structure, the resulting minimum vertical resolution is about 2 m.

Because there were an unusually high number (six) of clearly imaged S-wave reflectors as shown in Figures 2 and 3, and some uncertainty about picking refraction arrivals on the near offsets in the presence of a probable velocity inversion, we decided to interpret the site using only the reflection data. We based the presence of a near-surface velocity inversion on two travel-time features of the S-wave profile seen in Figure 3: 1) a refraction termination and time delay to the next higher velocity refraction arrival, and 2) the higher S-wave reflection velocity we interpreted in the upper 0.1 s of the data. The velocity-depth interpretation based on the reflection data was the result submitted for the blind comparison study and is shown in Figure 4 and Table 2. However, for the layer immediately below the deepest reflector we did assign a velocity equal to the highest velocity refraction detected (~490 m/s), which is shown in Figure 5. In this interpretation the velocities range from 155 m/s in a 2 m thick layer at the surface to about 490 m/s at 77 m depth. There are two low-velocity zones, one at 9 to 18 m depth and the other at 40 to 55 m depth, that distinguish the reflection interpretation from the purely refraction data interpretation described in the next paragraph. Using the S-wave reflection velocity-depth data and the NEHRP guidelines equation, we also calculated the average V_S to 30-m depth (V_{S30}) at 220 m/s.

As a check against the reflection-only S-wave interpretation we also analyzed the data strictly in terms of refraction arrivals (Fig. 5). For the refraction data we selected first-arrival phases, assumed to be refracted from the same interface, from an interactive video-screen display of the shot record. Velocity and the zero-offset time were then calculated from the slope of the line we fit to these phases. The zero-offset times and velocities were input to a computer program (Mooney, 1984) to generate a depth section. Seven layers were found by this technique with velocities increasing from about 160 m/s at the surface to about 490 m/s at about 80 m depth. Comparing the results of the two

4

interpretations we find that, except for the near surface zone to about 18 m depth, the layer velocities of the reflection and refraction data interpretations generally agree within 10 percent (Fig. 6). The V_{S30} values are also similar at 214 m/s and 220 m/s for the refraction and reflection data, respectively. An alternative method of determining V_{S30}, developed by Williams and others (2001), simply converts the 100 m offset S-wave travel-time, which is picked from the common-source point seismic record (Fig. 7), to velocity through an empirical relationship established from several measurements in California and Washington. In this approach the interpreter simply notes the travel time of the first arriving phase at the geophone placed 100 m from the seismic source (Fig. 7). The Vs30 value determined in this way is 211 m/s.

The P-wave seismic velocity profile was determined from travel-time features of the P-wave profile shown in Figure 8. We used the prominent direct arrivals and refractions in these records to pick 4 distinct layers in the upper 40 m. Poorly imaged reflections in the 0.25 to 0.3 s time range suggest the highest refraction velocity of 2081 m/s probably extends to a depth of about 230 m (Fig. 8). The top two layers have seismic velocities of 280 and 1285 m/s with thicknesses of 4 and 6 m, respectively (Fig. 9 and Table 3), and, given the relatively high velocity of the second layer, it is probably partially saturated. The abrupt termination of the refraction phase from the second layer suggests the presence of a low-velocity zone underlying the second layer that appears to correspond to an upper low-velocity zone observed in the S-wave interpretation. The thickness of this low-velocity zone was assigned to be 5 m, which is approximately the same thickness as the S-wave low-velocity zone. The velocity of the low-velocity zone was constrained to 900 m/s by maintaining the 5:1 P- to S-wave velocity ratio observed in the unconsolidated sediments of the overlying layer. This low-velocity zone probably acts as a ground water barrier that perches water in the second layer. The highest velocity layer interpreted appears to begin at about 15 m depth and extends to at least 40 m depth and possibly much deeper as described above when considering weak reflection data.

Discussion and Conclusions

We used reversed P- and S-wave seismic reflection/refraction profiles to measure the thickness and velocity of the upper 85 m near drillhole CCOC. These data were acquired as part of a study to compare different methodologies for measuring the seismic velocity structure at this site. We interpreted eight layers in the S-wave seismic profiles including two low-velocity zones. The upper low velocity zone was identified by a clear refraction termination and time delay to the next visible higher speed refraction. The deeper low-velocity zone, which also corresponds to a low-velocity zone in the P-wave result, was interpreted from the conversion of reflection stacking velocities to interval velocity and was not observed to have the associated refraction termination. Four layers were interpreted in the P-wave data including the low-velocity zone described above and a probable perched water bearing zone in the upper 4-10 m depth.

When comparing these results to the suspension log velocities measured in the CCOC hole, located about 200 m northwest of the center of the seismic profile, the reader should remember several factors that could cause differences in velocity between the two measurements. The first factor is simply the distance between the measurement sites and

possible differences in sedimentation. The second factor is the large horizontal area measured by seismic reflection/refraction profile, as compared to the suspension log, which would tend to filter and smooth the reflection/refraction data, giving a result that is more of an average over a larger area. Depending on the site characterization requirements, the reflection/refraction data result might be preferred because it measures a larger area, although with less detail. The third factor to consider is anisotropy. Because the seismic reflection/refraction wavefronts tend to propagate in a non-vertical direction through the media, and the suspension log procedure derives its result from vertically propagating waves, seismic velocity measured horizontally along the bedding can be 10-15 percent higher than velocity measured vertically as in a well (Sheriff, 1984). Considering all these factors, it is remarkable the two methods are comparable at all.

A final point to consider is that among all the methods applied at the CCOC site, we believe the seismic reflection/refraction method offers the most direct measure of the site's true impedance structure. Indeed, seismic reflections have been shown to directly correspond to independently recorded earthquake site resonances (Williams and others, 2000). Although there is some art and subjectivity involved in the interpretation of these data, it does have the advantage of avoiding complicated inversions which depend on a starting model that is basically a guess.

Acknowledgments

Table 1. Seismic-refraction/reflection data recording parameters.

Location:	South end of profile: N37.33464, W121.86740; north end: N37.33621, W121.86750
Recording system:	Geometrics Strata View 24-bit seismograph (60 channels)
Sampling interval:	0.001 seconds
Record length:	2 seconds
Recording format:	SEG-2
Geophones:	60, 4.5-Hz horizontal or 8-Hz vertical
Geophone array:	Linear with single phones at 3.0-m intervals
Source:	4.0-kg sledgehammer on wood timber (S-wave) or steel plate (P-wave)
Source array geometry:	Linear, 177-m array length

Table 2. S-wave velocity-depth result

Depth (m)	Velocity (m/s)
0-2	155
2-9	250
9-18	175
18-27	250
27-40	370
40-54	330
54-78	410
78-85	495

Table 3. P-wave velocity-depth result

Depth (m)	Velocity (m/s)
0-4	280
4-10	1285
10-15	900
15-40	2080

References

Campbell, K.W., Duke, C.M., 1976. Correlations among seismic velocity, depth and geology in the Los Angeles area. School of Engineering and Applied Science, UCLS, UCLA-ENG-7662. 54 pp.

Dobrin, M.B., 1976. Introduction to geophysical prospecting. McGraw-Hill Book Company, New York.

Harris, J., Street, R., Kiefer, D., Allen, D., Wang, Z., 1994. Modeling site response in the Paducah, Kentucky, area. Earthquake Spectra 10, 519-538.

King, K.W., Carver, D.L., Williams, R.A., Worley, D.M., Cranswick, E., Meremonte, M. E., 1990. Santa Cruz seismic investigations following the October 17, 1989 Loma Prieta Earthquake. U.S. Geol. Surv. Open-File Report 90-307, 59 pp.

Liberty, L., 1998. Seismic reflection imaging of a geothermal aquifer in an urban setting. Geophysics 63, 1285-1294.

Luzietti, E.A., Kanter, L.R., Schweig, E.S., Shedlock, K.M., Van Arsdale, R.B.,1992. Shallow deformation along the Crittenden County Fault zone near the southeastern boundary of the Reelfoot Rift, northeastern Arkansas. Seismol. Res. Lett. 63, 263-275.

Miller, R.D., Anderson, N.L., Feldman, H.R., Franseen, E.K., 1995. Vertical resolution of a seismic survey in stratigraphic sequences less than 100 m deep in southeastern Kansas. Geophysics 60, 423-430.

Mooney, H.M., 1984. Handbook of engineering geophysics, volume 1, seismic. Bison Instruments, Inc., Minneapolis, Minn.

Sheriff, R.E., 1984. Encyclopedic dictionary of exploration geophysics: Society of Exploration Geophysics, 323 p.

Steeples, D.W., 1998. Shallow seismic reflection section-introduction. Geophysics, Special Issue 63, 1210-1212.

Williams, R.A., Cranswick, E., King, K.W., Carver, D.L., Worley, D. M., 1994. Site-response models from high-resolution seismic reflection and refraction data recorded in Santa Cruz, California. In: Borcherdt, R.G. (Ed.), The Loma Prieta, California, Earthquake of October 17, 1989-Strong Ground Motion. U.S. Geol. Surv. Prof. Pap. 1551-A, A217-242.

Williams, R.A., Stephenson W.J., Frankel, A.D., Cranswick, E., Meremonte, M.E., and J.K. Odum, 2000, Correlation of 1- to 10-Hz earthquake resonances with surface measurements of P- and S-wave reflections and refractions in the upper 50 m: Bull. Seism. Soc. of Am., v 90, no. 5, p 1323-1331.

Williams, R.A., Stephenson, W.J., Frankel, A.D., and Odum, J.K., 2001. Using high-resolution surface seismic imaging to study earthquake site response. Geol. Soc. Am., Abstracts with Programs 33, A-345.

Williams, R.A., Stephenson W.J., Odum J.K., and Worley, D.M, 2003, Comparison of P- and S-wave velocity profiles from surface seismic refraction/reflection and downhole data: Contributions of High Resolution Geophysics to Understanding Neotectonic and Seismic Hazards, J.H. McBride and W.J. Stephenson, eds., Tectonophysics, v. 368, p. 71-88.
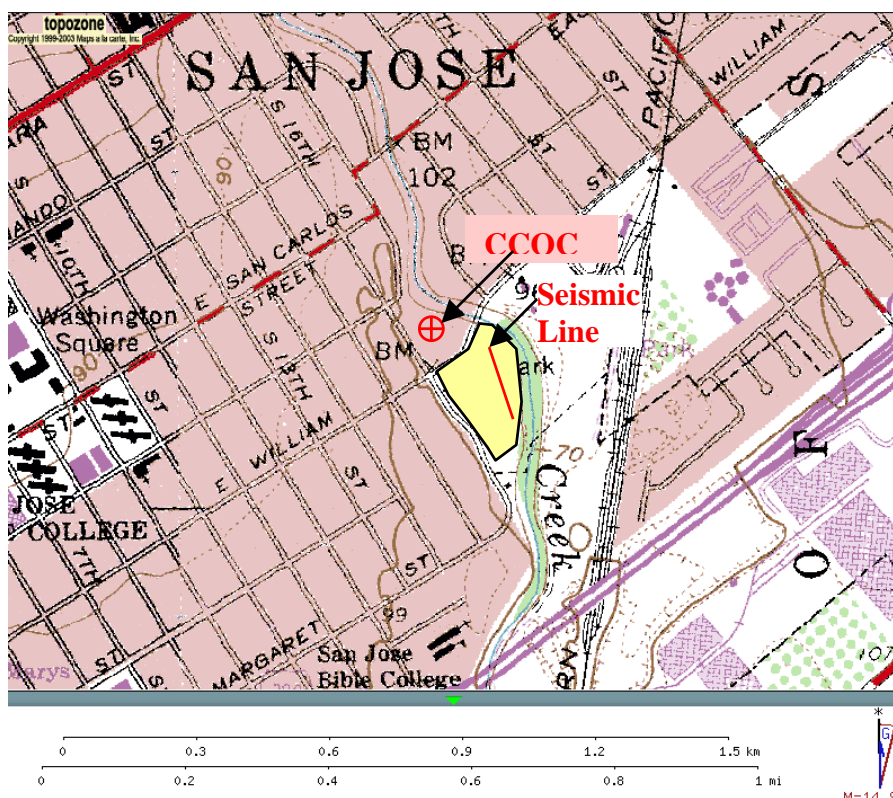
Figure 1. Location map showing the CCOC drill hole relative to the reflection/refraction profile site (red line) in William St. Park (yellow area).
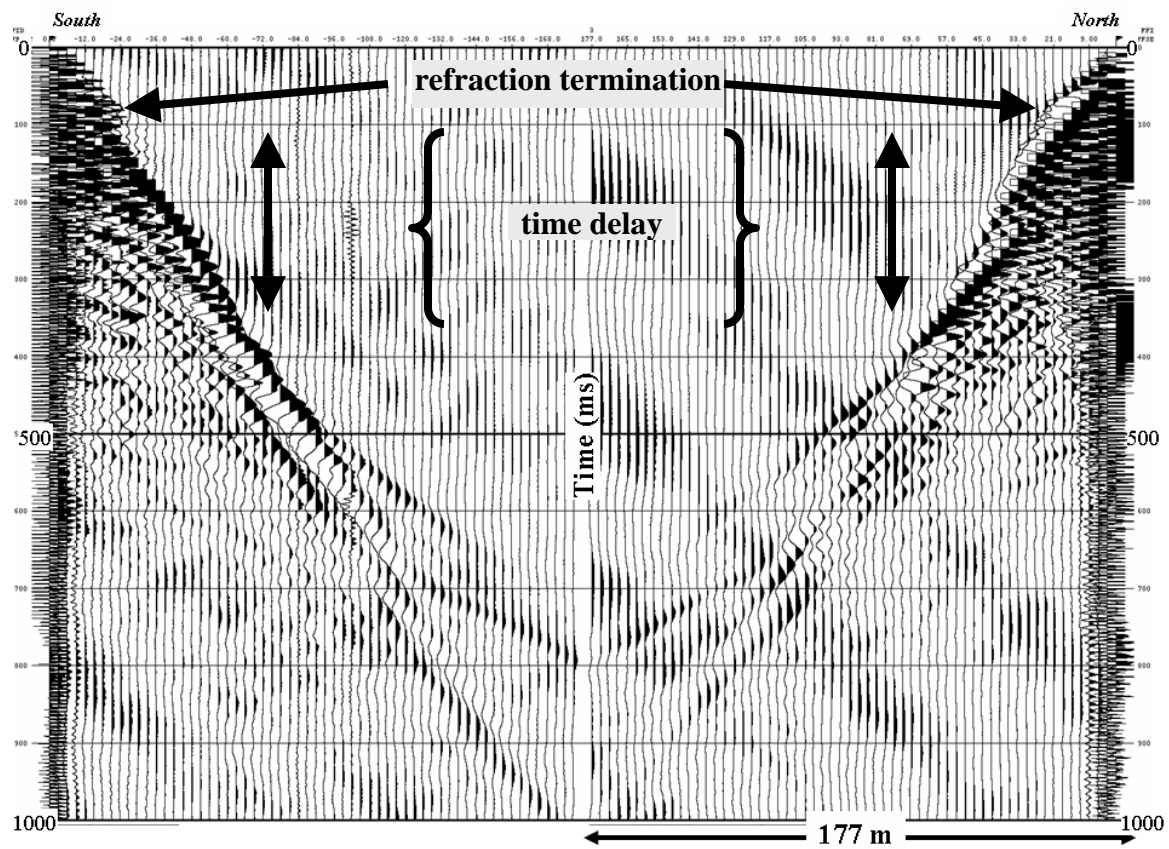
Figure 2. True amplitude display of reversed S-wave seismic profiles. No filters or gain have been applied to these data.
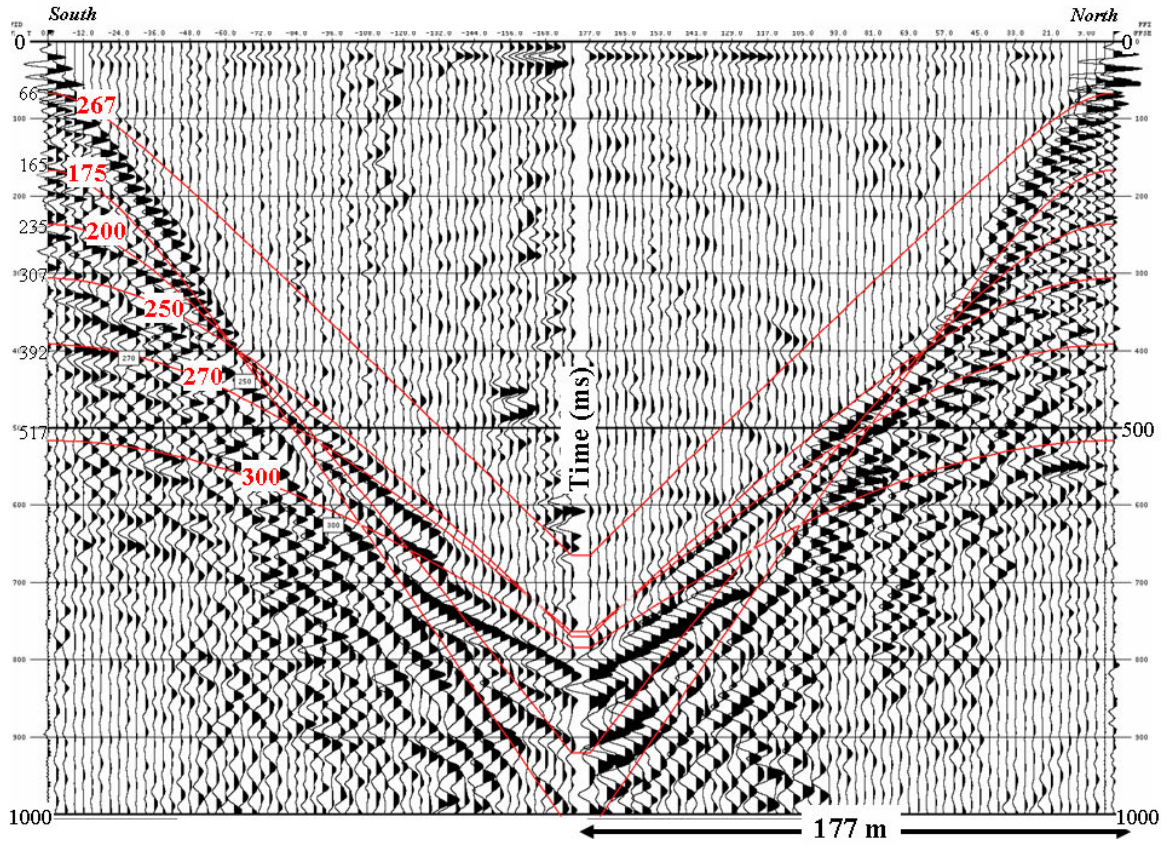
Figure 3. Data from Figure 2, filtered by a 15-25-60-100 Hz band pass and scaled by 100 ms automatic gain control (AGC), and showing the reflection interpretation (red lines), moveout velocities, and zero-offset times (black numbers on the left next to the zero-offset point of the fitted reflection hyperbola.
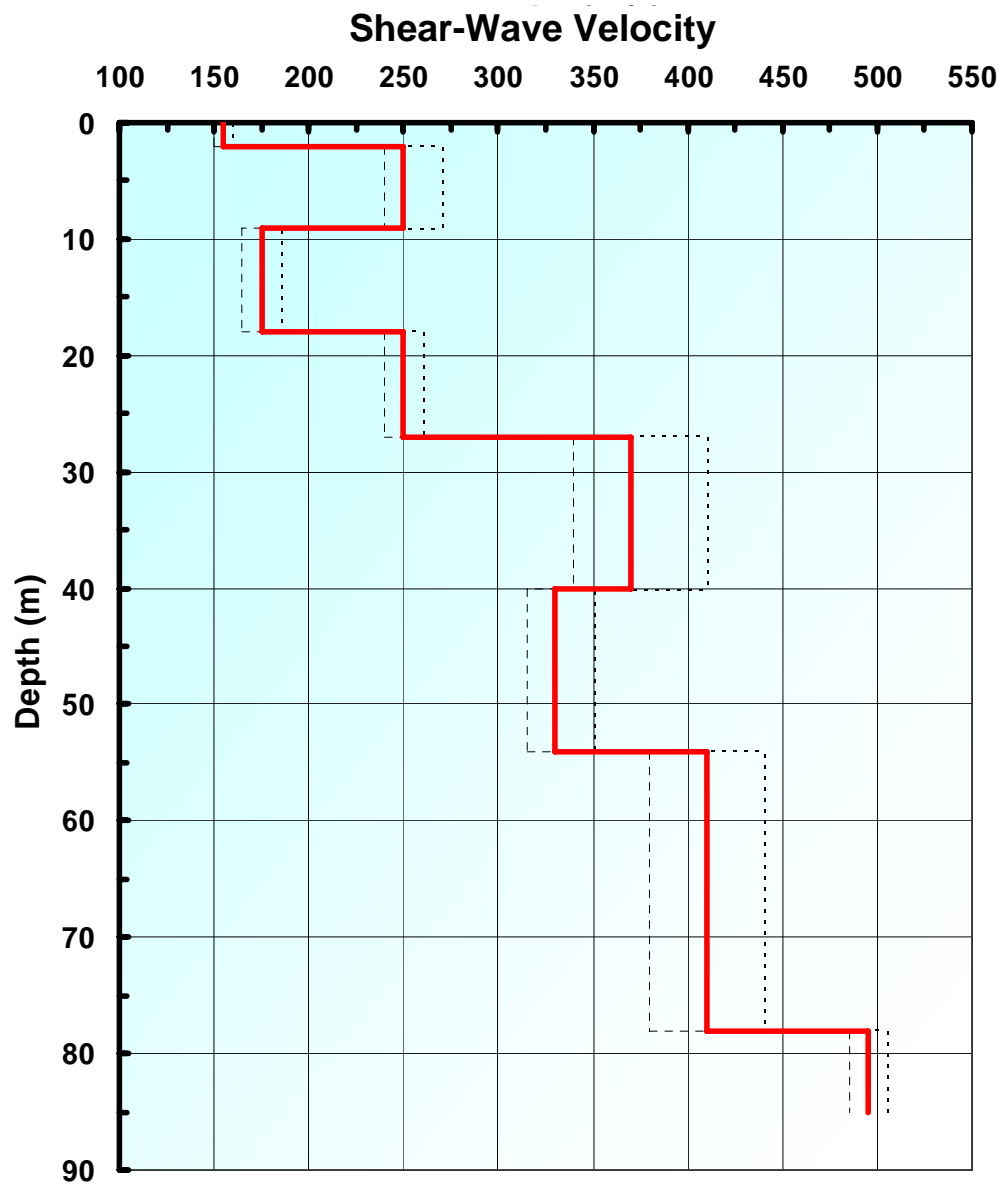
Figure 4. S-wave depth-velocity model resulting from interpretation of the reflection data (red line). Dashed lines show a tolerable range of velocities from the preferred value.
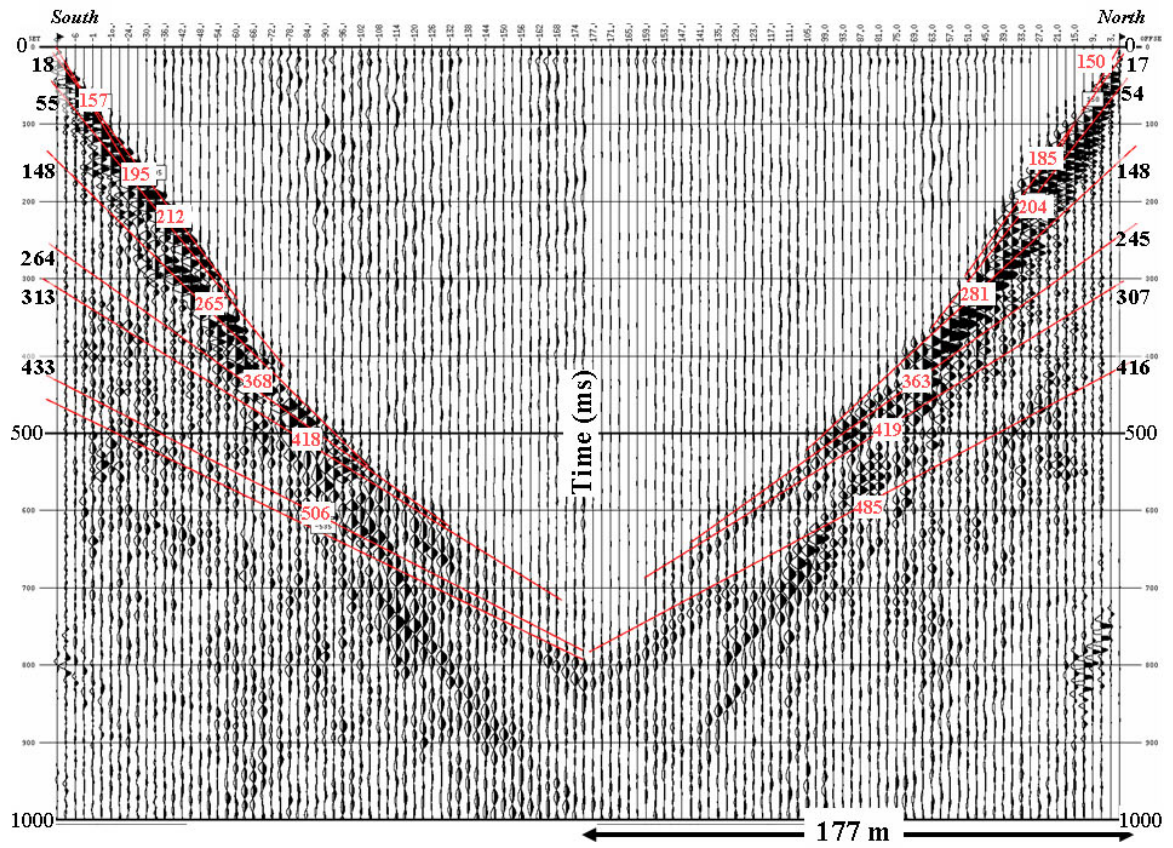
Figure 5. Reversed profiles showing S-wave travel times, refraction interpretation and the corresponding seismic velocities for those layers. These data were filtered by a 10-20-60-100 Hz bp and scaled by 350 ms window AGC.
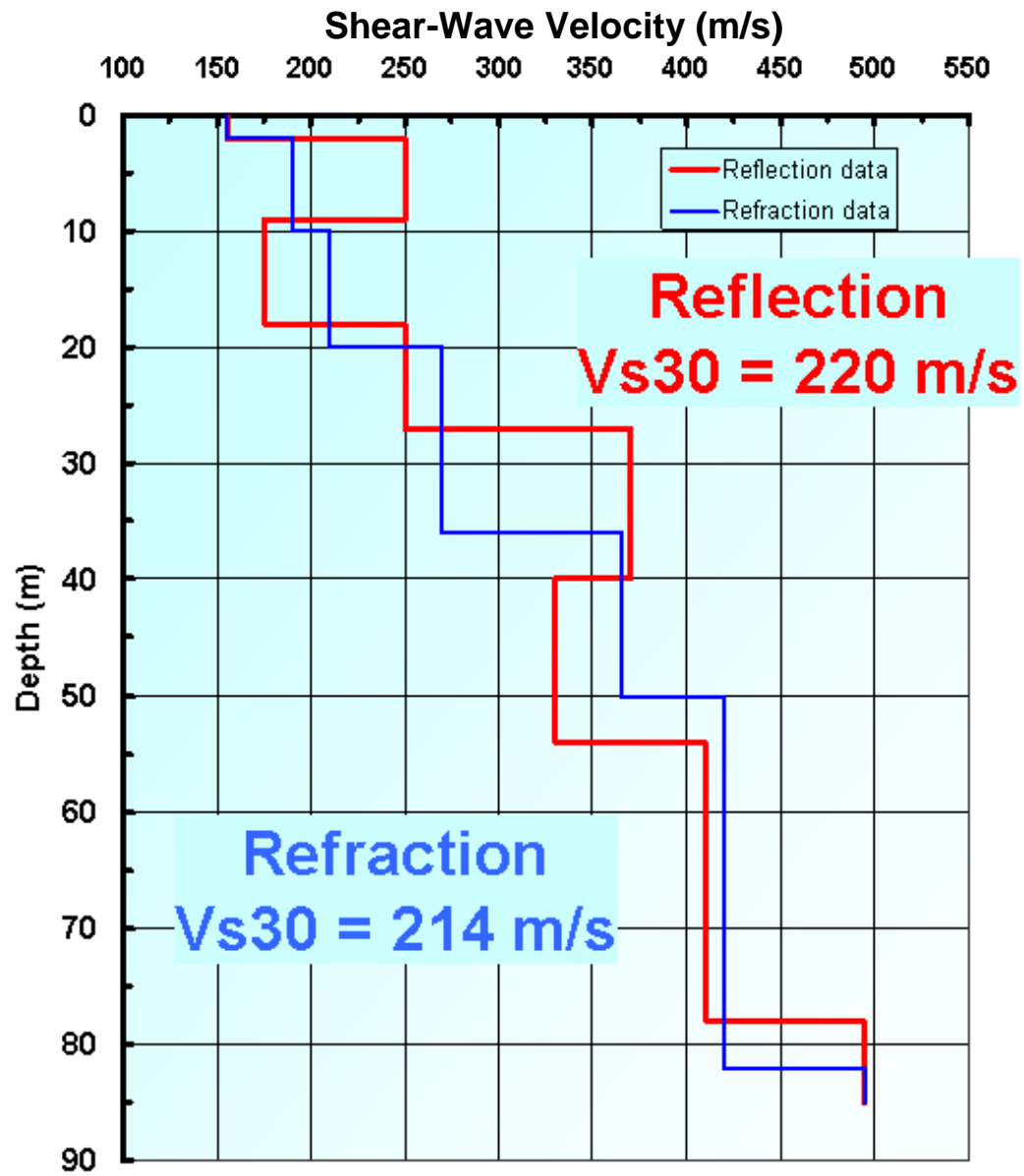
13

Figure 6. Comparison of seismic reflection and refraction profile depth-velocity profiles and their corresponding Vs30 values.
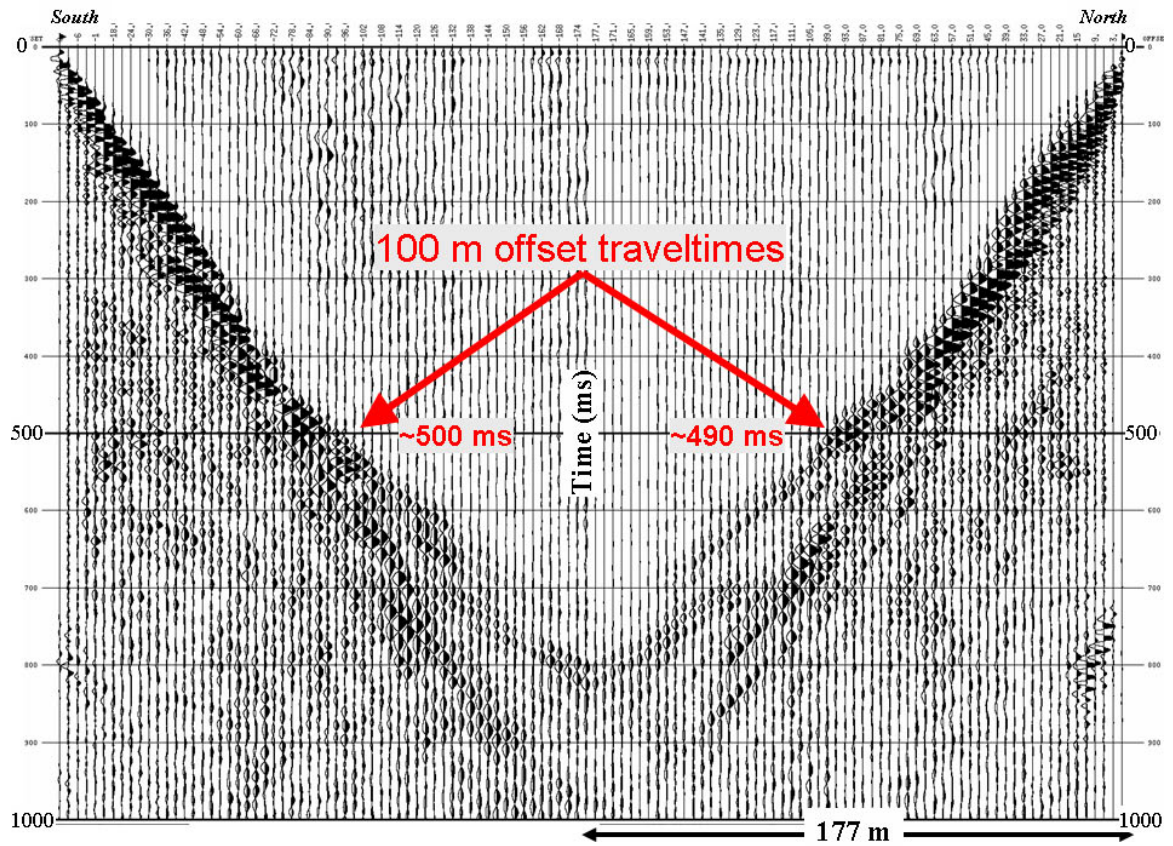
Figure 7. Data used to estimate Vs30 from S-wave travel times to 100 m offset distance from the seismic source.
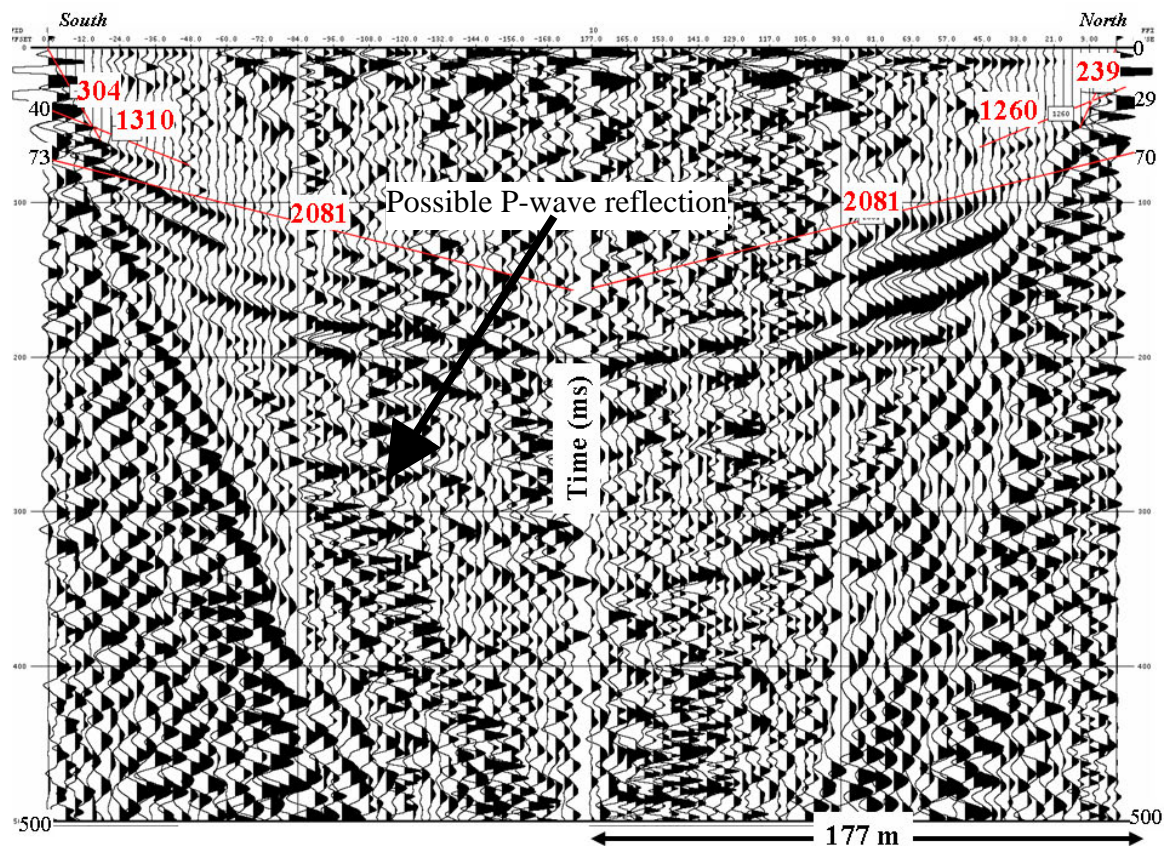
Figure 8. Reversed common source-point P-wave seismic records showing refraction slopes (red) and the velocity associated with that slope. These data were filtered by a 20-40-120-180 bandpass and scaled by a 100 ms AGC.
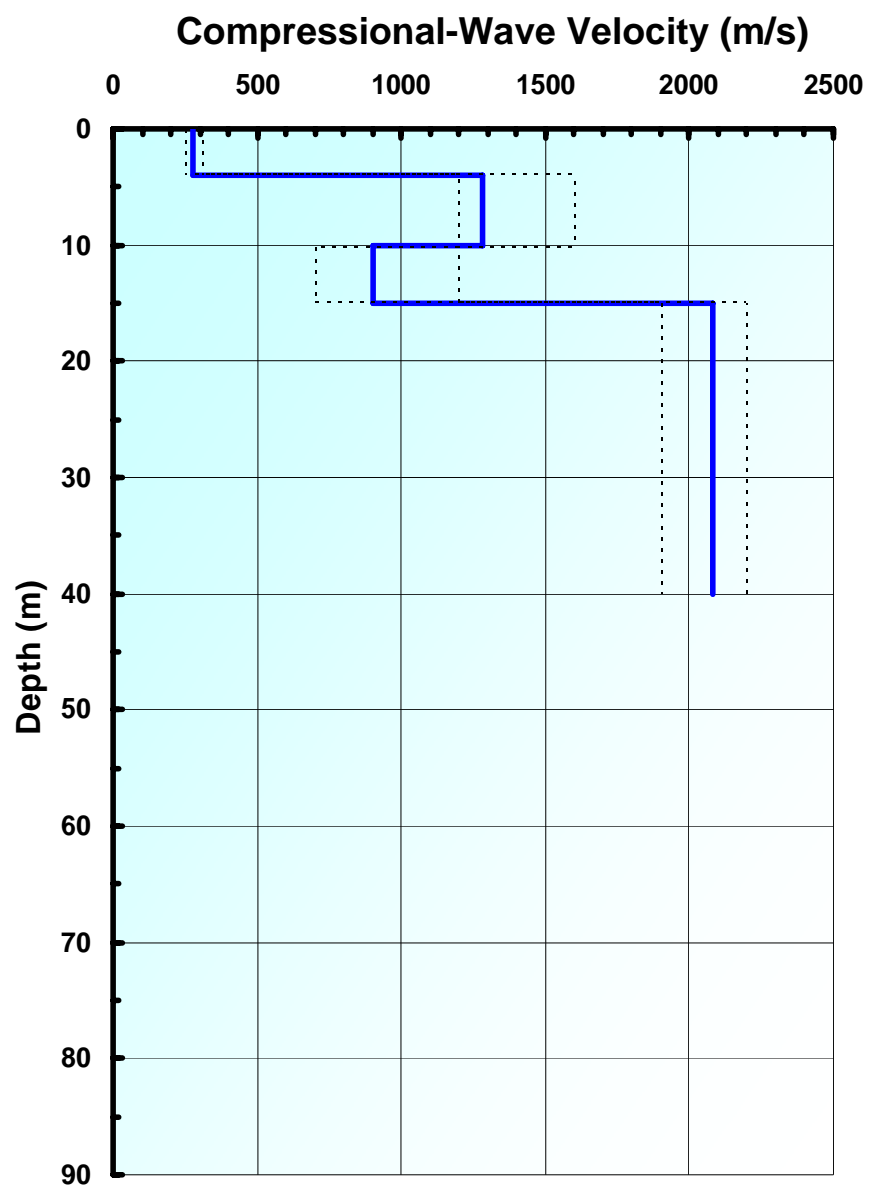
Figure 9. Depth-velocity model interpreted from P-wave seismic record shown in Figure 8.